



HAL
open science

Minimization of Parameter Sensitivity to Pre-Estimation Errors and its Application to the Calibration of Magnetometer Arrays

Raphaël Neymann, Hendrik Meier, Hugo Lhachemi, Christophe Prieur,
Antoine Girard

► **To cite this version:**

Raphaël Neymann, Hendrik Meier, Hugo Lhachemi, Christophe Prieur, Antoine Girard. Minimization of Parameter Sensitivity to Pre-Estimation Errors and its Application to the Calibration of Magnetometer Arrays. ECC 2023 - 21st European Control Conference, Jun 2023, Bucarest, Romania. 10.23919/ECC57647.2023.10178334 . hal-04072014

HAL Id: hal-04072014

<https://hal.science/hal-04072014v1>

Submitted on 17 Apr 2023

HAL is a multi-disciplinary open access archive for the deposit and dissemination of scientific research documents, whether they are published or not. The documents may come from teaching and research institutions in France or abroad, or from public or private research centers.

L'archive ouverte pluridisciplinaire **HAL**, est destinée au dépôt et à la diffusion de documents scientifiques de niveau recherche, publiés ou non, émanant des établissements d'enseignement et de recherche français ou étrangers, des laboratoires publics ou privés.

Copyright

Minimization of Parameter Sensitivity to Pre-Estimation Errors and its Application to the Calibration of Magnetometer Arrays

Raphaël Neymann^{1,2}, Hendrik Meier², Hugo Lhachemi¹, Christophe Prieur³, and Antoine Girard¹

Abstract—We consider the problem of parameters estimation in the situation where a subset of parameters of the underlying model has already been estimated. Potential errors in the pre-estimated parameters limit the accuracy in the computation of the still unknown parameters in a way that crucially depends on the symmetries of the data set. In this article, we develop an optimization approach that minimizes the sensitivity to errors in the determination of parameters by determining optimal weights that depend on both the model and the input data in the situation where the data are incomplete. We apply the method to the problem of calibrating the sensor positions in an array of magnetometers whose scale factors and biases have been estimated beforehand.

I. INTRODUCTION

Sensor calibration is an essential step to get acceptable performance from any navigation devices. Consistent measurements are constantly required in navigation algorithms, in particular in practical applications of *magneto-inertial dead-reckoning*, which consists in a fusion of inertial and magnetic measurements.

Fundamentally, a calibration is an optimization problem, for which the inputs are a dynamic data set and, often, additionally pre-estimated parameters, *e.g.*, physical constants or model parameters known or estimated beforehand. Inaccurate knowledge of these parameters can have a strong impact on the final calibration as the optimization problem can be very sensitive to their errors.

In the context of magnetic sensors, many calibration methods make use of the invariant associated with a homogeneous field, either the Earth's magnetic field [9], [10], [12], [20] or coil-generated constant field [5], [14], [15]. Calibrations in inhomogeneous fields have also been developed [1], [4], [18], [21]. It has recently [4] been proven that in inhomogeneous fields, positions of magnetometers become identifiable using a motion capture reference. The knowledge of this geometry is needed for the computation of the magnetic field gradient, which is the key ingredient within *magneto-inertial dead-reckoning* [2], [3], [19]. More recent developments include the combination of magneto-inertial algorithms with machine learning [22], [23] and magnetic mapping [8].

We are thus interested in calibrating the positions of the single-axis sensors in an array of magnetometers as accurately as possible. The full calibration model being highly

non-linear [4], typical calibration methods rely either on dynamic systems [16] or linearization and iteration, using Least-Squares methods (LS), especially Ordinary Least-Squares (OLS) that assign the same weight to each sample. However, in the latter case, iterating on inaccurate input parameters can lead to amplified errors in the final results. Moreover, trajectories used to generate calibration data often require particular symmetries in their design (needed for reducing the sensitivity in the pre-estimation errors), which may be yet hard to properly define and execute, especially if the sensors are embedded in a larger device.

In this paper, we develop a calibration algorithm that is resilient with respect to errors in the pre-estimated parameters and unexpected perturbations in the experiment by assigning suitable weights to the input samples. Our approach is inspired by the computation of a fictional material in magnetostatics for which the sensitivity in the magnetic permeability and electrical current is minimal [6], and aims to compute a sample-dependent weight function such that the estimation of a calibration parameter of interest be as insensitive as possible to errors in a pre-estimated set of parameters. A sensitivity minimization strategy, based on data selection, has recently been implemented in the context of Li-ion batteries calibration [7]. A complementary approach, rebuilding missing points in incomplete data set with polynomials, has also been suggested [17]. Our method is yet more general, for it consists in a weighting strategy by assigning a quality coefficient to each sample of the data set.

Thus, we introduce a sensitivity measure of the estimated parameters with respect to pre-estimation errors. This sensitivity can then be minimized by selecting an optimal weight function of the data set.

To demonstrate the utility, in Sec. II, we first study within a simple toy problem how selecting suitable subsets of the calibration data can significantly reduce the sensitivity in a simple situation. We then establish a general method in Sec. III applicable to situations in which exploitable symmetries are not evident and finally apply this method in Sec. IV to our initial problem of estimating the sensor positions in an array of magnetometers.

II. A TOY PROBLEM STUDY

In this section, we motivate our approach by showing on a simple toy problem that selecting or weighting the calibration can help to reduce the sensitivity to errors in pre-estimated parameters.

¹ Université Paris-Saclay, CNRS, CentraleSupélec, Laboratoire des Signaux et Systèmes, 91190 Gif-sur-Yvette, France

² SYSSNAV, 27200 Vernon, France

³ Université Grenoble Alpes, CNRS, Grenoble-INP, GIPSA- lab, 38000 Grenoble, France. The work of the second author has been partially supported by MIAI@Grenoble Alpes (ANR-19-P3IA-0003).

A. Model for a 2D magnetometer

Consider a single-axis sensor in a two-dimensional world measuring the projection of an ambient tangent field, *e.g.* a magnetic field, onto its axis. The sensor is attached to a (moving) body, to which a (moving) reference frame \mathbf{b} has already been assigned. If the sensor response to the ambient field \mathbf{B} is linear, a complete model for the measurement M is given by

$$M = \mathbf{c} \cdot \mathbf{B}^{\mathbf{b}} + b. \quad (1)$$

Herein, $b \in \mathbb{R}$ denotes the sensor bias, and the (row) vector $\mathbf{c} = (c_x \ c_y) \in \mathbb{R}^{1 \times 2}$ points along the sensitive axis (in body frame \mathbf{b}). Its norm is the scale factor. The upper index \mathbf{b} in $\mathbf{B}^{\mathbf{b}}$ indicates that vector components are in body frame.

Our objective is to have at our disposal the best possible estimates for the calibration parameters b and \mathbf{c} . Suppose that the bias b has already been estimated to a value b_0 by a separate calibration method, *e.g.*, in a zero-field chamber, with a residual error $\delta b = b_0 - b_*$, where b_* denotes the true but unknown bias value. In this situation, we wish to estimate the remaining calibration parameter \mathbf{c} while being as insensitive as possible to the potential error δb .

B. A simple calibration method

For the estimation of the scale factor vector \mathbf{c} , suppose the following experiment has been carried out: the rigid body carrying the sensor is rotated by a *known* angle θ with respect to the (inertial) navigation frame \mathbf{n} . The (uniform) ambient field is oriented along the y -axis of this frame, $\mathbf{B}^{\mathbf{n}} = (0 \ B)^\top$. In this situation, the (by hypothesis noise-free) measurement for a given θ amounts to

$$M(\theta) = \mathbf{c} \cdot R(\theta)^\top \mathbf{B}^{\mathbf{n}} + b \text{ with } R(\theta) = \begin{pmatrix} \cos \theta & -\sin \theta \\ \sin \theta & \cos \theta \end{pmatrix}, \quad (2)$$

cf. the models in [4] and [10] and Fig. 1.

If measurements $M(\theta)$ are available for homogeneously distributed angles $\theta \in (-\pi, \pi)$, a standard LS optimization of \mathbf{c} with b fixed to the possibly erroneous pre-estimate b_0 yields a value that is independent from the actual bias b , *cf.* Eq. (28) in App. V-A. This value is thus fully insensitive to any residual error δb , *i.e.* equal to the true value. This independence is a manifestation of the $O(2)$ rotational symmetry in the chosen samples.

If however, for some reason, measurements are available only for $\theta \in (-\frac{\pi}{4}, \frac{3\pi}{4})$, see Fig. 1, the aforementioned symmetry is broken and the standard LS optimization yields an error

$$\delta \mathbf{c} = \frac{\delta b}{B} \frac{2\sqrt{2}}{\pi} (1 \ -1), \quad (3)$$

using Eq. (30) of App. V-A. This error reflects how within the standard approach, the scale factor estimation is quite sensitive to residual errors in the pre-estimated bias b .

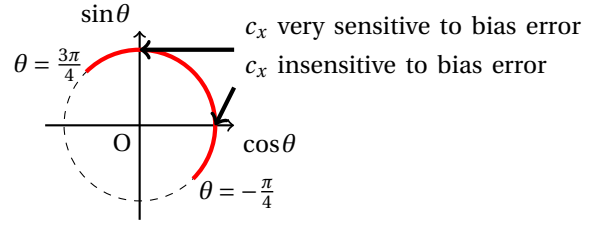


Fig. 1: In red the angles covered by the calibration experiment. The arrows indicate the regions within this trajectory where the scale factor c_x is very sensitive or insensitive to an error in the pre-estimated bias b , *cf.* Eqs. (4) and (5). (For c_y , the regions of high and low sensitivities are simply reversed.)

C. Sensitivity in data subsets

For the trajectory $\theta \in (-\frac{\pi}{4}, \frac{3\pi}{4})$, the result obtained by standard LS calibration contains an error of order $\delta b/B$. Let us now consider the subset of the initial trajectory given by $\theta \in (-\varepsilon, \varepsilon)$ for $0 \leq \varepsilon \leq \pi/4$. Applying the LS optimization to this interval only, we obtain, using again Eq. (30), the scale factor vector up to an error

$$\delta \mathbf{c} = \frac{\delta b}{B} (0 \ \iota(\varepsilon)), \quad (4)$$

with $\iota(\varepsilon) = (2 \sin \varepsilon) / (\varepsilon + \sin \varepsilon \cos \varepsilon)$ taking values between 1 and ≈ 1.1 . Whereas the error δc_y remains of order $\delta b/B$, the estimation of c_x is remarkably insensitive to the error δb in the pre-estimated bias, see Fig. 1. This insensitivity can be attributed to the reflectional symmetry (w.r.t. $\theta = 0$) of the subset of calibration data.

Analogously, for θ close to $\pi/2$, *i.e.* $\theta \in (\frac{\pi}{2} - \varepsilon, \frac{\pi}{2} + \varepsilon)$, we find the error estimate

$$\delta \mathbf{c} = \frac{\delta b}{B} (\iota(\varepsilon) \ 0). \quad (5)$$

Here, c_x , with an error of order $\delta b/B$, is very sensitive to δb , see Fig. 1, as the reflectional symmetry (w.r.t. $\theta = \pi/2$) favors c_y , whose error vanishes.

As a result, we find that the LS sensitivity of the estimation of each calibration parameter to the error in the pre-estimated parameters depends crucially on the underlying input data. In particular, symmetries within a well-chosen subset of input data may render a certain parameter insensitive to such errors.

Following the small toy model study of this section, we develop in Sec. III a general approach to minimize the sensitivity of parameter estimation to errors in pre-estimated parameters in situations in which exploitable symmetries are not apparent.

III. GENERAL APPROACH

In this section, we propose a general approach for an optimization problem estimating (calibration) parameters with minimal sensitivity to errors in predetermined parameters.

A. Setting of the problem

We consider a sensor calibration problem defined by its involved quantities and a calibration model of the form defined below.

Definition 1: Physical quantities. A calibration problem involves

- the *calibration parameter vector* $\boldsymbol{\pi} \in \mathbb{R}^n$, $n \in \mathbb{N}^*$, to be estimated;
- a *vector of pre-estimated calibration parameters* $\mathbf{m}_0 \in \mathbb{R}^m$, $m \in \mathbb{N}^*$, needed for the estimation of $\boldsymbol{\pi}$ and determined with known precision characterized by a given covariance matrix;
- a set of *data points* $k \in \{1, \dots, N\} \mapsto \boldsymbol{\xi}_k \in \mathcal{M}$, where \mathcal{M} is the manifold in which the data points are recorded (*i.e.* data of the sensor to be calibrated and possibly other sensors used in the calibration experiment).

Definition 2: Calibration model. A calibration model is a real-valued (C^3 -)function

$$\psi : \begin{cases} \mathbb{R}^n \times \mathbb{R}^m \times \mathcal{M} & \longrightarrow & \mathbb{R} \\ (\boldsymbol{\pi}, \mathbf{m}, \boldsymbol{\xi}) & \longmapsto & \psi(\boldsymbol{\pi}; \mathbf{m}, \boldsymbol{\xi}). \end{cases} \quad (6)$$

such that for the true value \mathbf{m}_* of the pre-estimated parameters, there is exactly one parameter vector $\boldsymbol{\pi}_*$ such that $\psi(\boldsymbol{\pi}_*; \mathbf{m}_*, \boldsymbol{\xi}) = 0$ for all $\boldsymbol{\xi} \in \mathcal{M}$.

B. Calibration formalism

For fixed pre-estimated parameters \mathbf{m}_0 and measurement data points $\boldsymbol{\xi}_k$, $k \in \{1, \dots, N\}$, we seek to estimate $\boldsymbol{\pi}$ by minimizing loss-function

$$\mathcal{J}_{\mathbf{m}_0, \boldsymbol{\xi}, f} : \begin{cases} \mathbb{R}^n & \longrightarrow & \mathbb{R}_+ \\ \boldsymbol{\pi} & \longmapsto & \Psi(\boldsymbol{\pi}, \mathbf{m}_0, \boldsymbol{\xi}, f), \end{cases} \quad (7)$$

with

$$\Psi(\boldsymbol{\pi}, \mathbf{m}_0, \boldsymbol{\xi}, f) = \sum_{k=1}^N f_k \psi(\boldsymbol{\pi}; \mathbf{m}_0, \boldsymbol{\xi}_k)^2, \quad (8)$$

Herein, the coefficients $f = (f_k)_{k=1, \dots, N}$ denote *weights* associated to each data point. They are defined by

Definition 3: Weight function. A weight function

$$k \in \{1, \dots, N\} \longmapsto f_k \in \mathbb{R}_+ \quad (9)$$

is a nonnegative function that satisfies the L^1 -property, $\sum_k f_k = 1$.¹

In the following, we develop the formalism that allows us to determine an optimal weight function f in order for the minimum of $\mathcal{J}_{\mathbf{m}_0, \boldsymbol{\xi}, f}$, which we denote $\hat{\boldsymbol{\pi}}_{|\mathbf{m}_0, \boldsymbol{\xi}, f}$, to have minimal sensitivity to errors in \mathbf{m}_0 .

We assume that $\hat{\boldsymbol{\pi}}_{|\mathbf{m}_0, \boldsymbol{\xi}, f}$ is (at least locally) a unique minimum and that the Hessian matrix of $\Psi(\boldsymbol{\pi}, \mathbf{m}_0, \boldsymbol{\xi}, f)$ w.r.t. $\boldsymbol{\pi}$ is positive definite at $\hat{\boldsymbol{\pi}}_{|\mathbf{m}_0, \boldsymbol{\xi}, f}$ for all weight functions f involved.²

¹In particular, *Ordinary Least-Squares* (OLS) correspond to $f = 1/N$.

²In practice, this can usually be accomplished with a sufficiently rich calibration trajectory.

C. Parameter sensitivity

We define the sensitivity of the unique minimum $\hat{\boldsymbol{\pi}}_{|\mathbf{m}_0, \boldsymbol{\xi}, f}$ as the linear response to the error $\mathbf{m}_0 - \mathbf{m}_*$ with respect to the true value \mathbf{m}_* of the pre-estimated parameter.

Definition 4: Parameter sensitivity. The sensitivity of the estimated parameter $\hat{\boldsymbol{\pi}}_{|\mathbf{m}, \boldsymbol{\xi}, f}$ to errors in the pre-estimated parameters \mathbf{m} , for given data $\boldsymbol{\xi}$ and weight function f , is defined as the derivative (Jacobian)

$$S_{\mathbf{m}_*, \boldsymbol{\xi}, f}(\hat{\boldsymbol{\pi}}) = \nabla_{\mathbf{m}} \hat{\boldsymbol{\pi}}_{|\boldsymbol{\xi}, f}(\mathbf{m}_*) \quad (10)$$

such that the error in $\hat{\boldsymbol{\pi}}_{|\mathbf{m}_0, \boldsymbol{\xi}, f}$ is given by

$$S_{\mathbf{m}_*, \boldsymbol{\xi}, f}(\hat{\boldsymbol{\pi}}) \cdot (\mathbf{m}_0 - \mathbf{m}_*) + O(\|\mathbf{m}_0 - \mathbf{m}_*\|^2). \quad (11)$$

With full knowledge of the system, the sensitivity can be readily computed from the loss function Ψ :

Proposition 1: The sensitivity $S_{\mathbf{m}_*, \boldsymbol{\xi}, f}(\hat{\boldsymbol{\pi}})$ is given by

$$S_{\mathbf{m}_*, \boldsymbol{\xi}, f}(\hat{\boldsymbol{\pi}}) = -H_{\boldsymbol{\pi}, \boldsymbol{\pi}}^{-1} \cdot H_{\boldsymbol{\pi}, \mathbf{m}}, \quad (12)$$

with the Hessian matrices

$$H_{\boldsymbol{\pi}, \boldsymbol{\pi}} = \nabla_{\boldsymbol{\pi}, \boldsymbol{\pi}}^2 \Psi(\hat{\boldsymbol{\pi}}_{|\boldsymbol{\xi}, f}(\mathbf{m}_*), \mathbf{m}_*, \boldsymbol{\xi}, f) \in \mathbb{R}^{n \times n},$$

$$H_{\boldsymbol{\pi}, \mathbf{m}} = \nabla_{\boldsymbol{\pi}, \mathbf{m}}^2 \Psi(\hat{\boldsymbol{\pi}}_{|\boldsymbol{\xi}, f}(\mathbf{m}_*), \mathbf{m}_*, \boldsymbol{\xi}, f) \in \mathbb{R}^{n \times m}.$$

Proof: The formula follows immediately from the implicit function theorem applied to the mapping

$$(\boldsymbol{\pi}, \mathbf{m}) \mapsto \nabla_{\boldsymbol{\pi}} \Psi(\boldsymbol{\pi}, \mathbf{m}, \boldsymbol{\xi}, f)$$

in the neighborhood of $(\hat{\boldsymbol{\pi}}_{|\mathbf{m}_*, \boldsymbol{\xi}, f}, \mathbf{m}_*)$. The Hessian $H_{\boldsymbol{\pi}, \boldsymbol{\pi}}$ is invertible by assumption, see Sec. III-B. ■

As the exact value \mathbf{m}_* is not known in our calibration, we may use the available (pre-)estimation \mathbf{m}_0 to obtain the approximation

$$S_{\mathbf{m}_*, \boldsymbol{\xi}, f}(\hat{\boldsymbol{\pi}}) \simeq S_{\mathbf{m}_0, \boldsymbol{\xi}, f}(\hat{\boldsymbol{\pi}}), \quad (13)$$

which, if inserted into Eq. (11), yields an equal error estimate of the same order. $S_{\mathbf{m}_0, \boldsymbol{\xi}, f}(\hat{\boldsymbol{\pi}})$ can be calculated from the Hessian matrices at \mathbf{m}_0 .

The i -th row of $S_{\mathbf{m}_0, \boldsymbol{\xi}, f}(\hat{\boldsymbol{\pi}})$ defines the sensitivity of the i -th component of $\boldsymbol{\pi}$ to the error in \mathbf{m}_0 . We denote by \mathbf{e}_i the i -th (row) vector of the standard basis of \mathbb{R}^n and thus obtain

$$s_{\mathbf{m}_0, \boldsymbol{\xi}, f}^{(i)}(\hat{\boldsymbol{\pi}}) = \mathbf{e}_i \cdot S_{\mathbf{m}_0, \boldsymbol{\xi}, f}(\hat{\boldsymbol{\pi}}) \quad (14)$$

as the sensitivity of the i -th component of $\boldsymbol{\pi}$.

Definition 5: Scalar sensitivity. The scalar sensitivity of the i -th component of $\hat{\boldsymbol{\pi}}_{|\mathbf{m}, \boldsymbol{\xi}, f}$ to errors in \mathbf{m} for data $\boldsymbol{\xi}$ and weight function f is defined as

$$\Lambda^{(i)}(f) = \left\| s_{\mathbf{m}_0, \boldsymbol{\xi}, f}^{(i)}(\hat{\boldsymbol{\pi}}) \right\|^2 \quad (15)$$

We assume that all components of \mathbf{m} have the same physical dimensions, which can always be achieved if necessary by applying suitable scale factors. We furthermore assume that the covariance matrix, which characterizes precision of the estimate \mathbf{m}_0 , is proportional to the unit matrix. This also is always achievable through a suitable orthogonal transformation and suitable scale factors.

Using Def. 5, we formulate the calibration problem as the following nonlinear variational problem: *Find a weight function $\hat{f}^{(i)}$ that minimizes $\Lambda^{(i)}(f)$.*

With an optimal weight function $\hat{f}^{(i)}$ at hand, the i -th component of $\boldsymbol{\pi}$ can be found by a LS optimization of $\boldsymbol{\pi}$. Depending on the situation, it may be suitable to treat several components at once by minimizing the sum of the corresponding (possibly weighted) functions $\Lambda^{(i)}(f)$ with respect to a common f .

D. Steps of the calibration algorithm

We summarize the steps the general method of calibration with minimal sensitivity to pre-estimated parameters.

- 1) Formulate the calibration problem as in the form of Sec. III-A.
- 2) Calculate the sensitivity $S_{\mathbf{m},\xi,f}(\hat{\boldsymbol{\pi}})$ using Proposition 1.
- 3) For the selected component (or components) i of the parameter vector $\boldsymbol{\pi}$, compute the optimal weight function \hat{f} by minimizing the sensitivity $\Lambda^{(i)}(f)$ of Eq. (15).
- 4) Compute $\hat{\boldsymbol{\pi}}|_{\xi,f}(\mathbf{m}_0)$ using the derivation by LS optimization using the optimal weight function \hat{f} .

For numerical optimizations discussed in this Article, we have used the Levenberg-Marquardt algorithm [11][13].

E. The toy problem revisited

To demonstrate the general approach, let us apply it to the toy-model of Sec. II. The quantities involved are $\boldsymbol{\pi} = \mathbf{c}$ (scale factor vector)³, $\mathbf{m} = b$ (pre-estimated bias), and $\boldsymbol{\xi}_k = (M(\theta_k), \theta_k)$ with $M_k = M(\theta_k)$ denoting the measurement at orientation angle θ_k . The calibration model is given by the function

$$\psi(\mathbf{c}, b, (M, \theta)) = M - b - Bc_x \sin \theta - Bc_y \cos \theta, \quad (16)$$

with B denoting the external field strength, cf. Eq. (2).

Calculating the Hessian matrices required for Proposition 1, we find for the sensitivity

$$\frac{\partial}{\partial b} \hat{\mathbf{c}}|_{(M,R),f}(b_0) = -H_{\mathbf{c},\mathbf{c}}^{-1} \cdot H_{b,\mathbf{c}} \quad (17)$$

with

$$H_{\mathbf{c},\mathbf{c}} = -\frac{B^2}{2} \sum_{k=1}^N f_k \begin{pmatrix} 1 - \cos 2\theta_k & \sin 2\theta_k \\ \sin 2\theta_k & 1 + \cos 2\theta_k \end{pmatrix}, \quad (18)$$

$$H_{\mathbf{c},b} = B \sum_{k=1}^N f_k \begin{pmatrix} \sin \theta_k \\ \cos \theta_k \end{pmatrix}. \quad (19)$$

For a given weight function, the scale factor estimate is

$$\hat{\mathbf{c}}|_{(M,R),f}(b_0) = -H_{\mathbf{c},\mathbf{c}}^{-1} \cdot B \sum_{k=1}^N f_k (M_k - b_0) \begin{pmatrix} \sin \theta_k \\ \cos \theta_k \end{pmatrix}, \quad (20)$$

which we note to be linear in b_0 . The error estimate $\widehat{\delta \mathbf{c}} = \delta b \cdot (\partial \hat{\mathbf{c}} / \partial b)$ is thus equal to the exact error $\delta \mathbf{c}$.

In the simulated calibration problem under consideration, a set of $N = 400$ data points is available for angles θ

³In this section, we consider \mathbf{c} to be a column vector.

TABLE I: Numerical results for errors and sensitivities for the calibration of c_i , $i = x, y$, for the homogeneous weights (OLS) and optimized weights LS obtained by symmetry considerations or by Levenberg-Marquardt (LM) optimization.

	OLS	Optimized weights	
		Symmetry	LM
Error δc_i (-)	$1.8 \cdot 10^{-4}$	$< 10^{-9}$	$< 2 \cdot 10^{-13}$
Scalar sensitivity $[\Lambda^{(x)}]^{1/2} (G^{-1})$	$0.9 \approx \frac{2\sqrt{2}}{\pi}$	$< 2 \cdot 10^{-6}$	$< 10^{-9}$

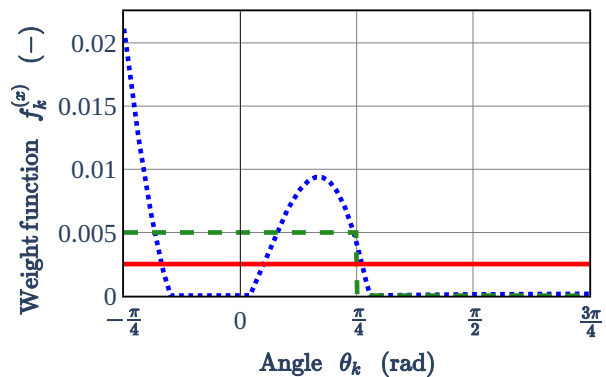


Fig. 2: OLS (red, solid) and optimized weights LS for the calibration of c_x in the toy-model. The optimal functions depicted are the one suggested by symmetry considerations (green, dashed) and the result of the LM optimization (blue, dotted).

distributed homogeneously over the interval $(-\pi/4, 3\pi/4)$. We choose the true values to be $\mathbf{c}_* = (0.0, 1.2)$, $b_* = 0.0$ G and $B = 1.0$ G while supposing a pre-estimated bias of $b_0 = 0.2$ mG.

Applying the approach of the previous section, we optimize the weight function f_k for c_x and c_y separately. For c_x ,⁴ we thus compute the weight function $\hat{f}_k^{(x)}$ that minimizes $\Lambda^{(x)} = |(1 \ 0) \cdot H_{\mathbf{c},\mathbf{c}}^{-1} \cdot H_{b,\mathbf{c}}|^2$.

For the numeric optimization, we employ a Levenberg-Marquardt (LM) algorithm, starting with homogeneous weights $f_k = 1/N$ for which the scalar sensitivity $[\Lambda^{(x)}]^{1/2}$ is of order 1 G^{-1} , see Table I. As result of the LM optimization, we obtain the non-trivial weight function $\hat{f}_k^{(x)}$ depicted in Fig. 2 and for which the sensitivity practically vanishes. Evaluating c_x using Eq. (20) with the optimal LM weights, we thus find the true value with practically vanishing error.

We further note that there is more than one optimal weight function. For instance, the much simpler weight

⁴For c_y , a completely analogous treatment yields the same results for sensitivity and error.

function given by $\hat{f}_k^{(x)} = 2/N$ for $\theta_k \in (-\pi/4, \pi/4)$ and $\hat{f}_k^{(x)} = 0$ otherwise, see Fig. 2, yields (practically) zero sensitivity and error as well (column ‘‘Symmetry’’ in Table I). It is this weight function that, chosen by symmetry considerations, has led to Eq. (4) in Sec. II-C.

For a good choice of a proper weight function in real situations, noise can be a factor that may favor some weight functions over others that are equally optimal in the noise-free setting.

IV. GEOMETRY OF AN ARRAY OF MAGNETIC SENSORS

The estimation of the magnetic gradient is an important ingredient of magneto-inertial navigation [19] and, if realized in an array of magnetometers, requires accurate knowledge of the array geometry, in particular the positions of the single sensors.

As recently shown by Chesneau *et al.* [4], it is possible to calibrate simultaneously for one single-axis magnetometer its scale factor, bias, and position relative to a body frame origin for which motion capture data are available. Being able to calibrate a single sensor in this way, we are *a fortiori* in a position to calibrate an array of such sensors. The calibration requires a trajectory providing as many independent observations than the number of parameters to estimate, and encompassing a region of space with an inhomogeneous magnetic field. In practice, it may become a difficult task to produce a trajectory that excites all the degrees of freedom necessary to identify all involved calibration parameters at once.

Here, we suppose that sensor scale factors and biases are known beforehand. This may be the case if a separate calibration, *e.g.* in a homogeneous magnetic field [10], has already been carried out or if an iterative calibration algorithm is used alternating scale factor and bias optimization on one hand and position optimization on the other hand. Furthermore, we assume that a local fit of the ambient magnetic field to a suitable model is available.

A. Formulation of the calibration model

We adopt the calibration model of [4] for the single-axis magnetometer

$$M - b - \mathbf{c} \cdot R^\top \hat{\mathbf{B}}^n(\mathbf{X} + R\mathbf{p}) = 0. \quad (21)$$

Herein, $\mathbf{p} \in \mathbb{R}^3$ is the sensor position in body frame relative to the frame origin, which is the parameter to be estimated: $\boldsymbol{\pi} = \mathbf{p}$. The sensor bias $b \in \mathbb{R}$ and scale factor (row) vector $\mathbf{c} \in \mathbb{R}^{1 \times 3}$ are the pre-estimated parameter: $\mathbf{m} = (b \ \mathbf{c})^\top$. Finally, we dispose for each data point of the sensor measurement $M \in \mathbb{R}$ as well as the position $\mathbf{X} \in \mathbb{R}^3$ of the body origin in the navigation frame \mathbf{n} and the attitude $R \in \text{SO}(3)$ of the rigid body relative to \mathbf{n} . These quantities together form the variable $\boldsymbol{\xi} = (M, \mathbf{X}, R) \in \mathcal{M} = \mathbb{R} \times \mathbb{R}^3 \times \text{SO}(3)$. Equation (21) with these definitions sets up a calibration problem in the sense of Sec. III-A.

As mentioned before, we suppose the magnetic field to be known in form of a map $\mathbf{X} \mapsto \hat{\mathbf{B}}^n(\mathbf{X})$. Assuming

positions \mathbf{p} close to the body origin on the scale defined the (non-linear) variations in the magnetic field, we obtain the calibration model $\psi : \mathbb{R}^3 \times \mathbb{R}^4 \times (\mathbb{R} \times \mathbb{R}^3 \times \text{SO}(3)) \rightarrow \mathbb{R}$ with

$$\psi(\mathbf{p}, (b, \mathbf{c}), (M, \mathbf{X}, R)) = M - b - \mathbf{c} \cdot R^\top [\hat{\mathbf{B}}^n(\mathbf{X}) + \nabla \hat{\mathbf{B}}^n(\mathbf{X}) R \mathbf{p}] \quad (22)$$

by linearization of Eq. (21).

In order to obtain a uniform physical dimension in the tuple $\mathbf{m} = (b \ \mathbf{c})^\top$, we may choose to measure the bias in units of the average magnetic field norm B .⁵

B. Computation of sensitivity

Using the method presented in Sec. III, our objective is to estimate the sensor position, obtained by LS minimization as

$$\hat{\mathbf{p}}|_{(M, \mathbf{X}, R), f}(b_0, \mathbf{c}_0) = -H_{\mathbf{p}, \mathbf{p}}^{-1} \cdot \sum_{k=1}^N f_k [M_k - b_0 - \mathbf{c}_0 \cdot R_k^\top \hat{\mathbf{B}}^n(\mathbf{X}_k)] R_k^\top \nabla \hat{\mathbf{B}}^n(\mathbf{X}_k) R_k \cdot \mathbf{c}_0^\top \quad (23)$$

for an optimal weight function f_k .⁶

Separating the sensitivities errors in bias and errors in the scale factor,

$$\frac{\partial}{\partial b} \hat{\mathbf{p}}|_{(M, \mathbf{X}, R), f}(b_0, \mathbf{c}_0) = -H_{\mathbf{p}, \mathbf{p}}^{-1} \cdot H_{\mathbf{p}, b} \quad (24)$$

$$\nabla_{\mathbf{c}} \hat{\mathbf{p}}|_{(M, \mathbf{X}, R), f}(b_0, \mathbf{c}_0) = -H_{\mathbf{p}, \mathbf{p}}^{-1} \cdot H_{\mathbf{p}, \mathbf{c}}, \quad (25)$$

we set up three cost functions, for each of the components of $\mathbf{p} = (p_x, p_y, p_z)^\top$ in the form

$$\Lambda^{(i)}(f) = \sigma_b^2 \left(\frac{\partial \hat{p}_i}{\partial b} \Big|_{(M, \mathbf{X}, R), f} \right)^2 + \sigma_{\mathbf{c}}^2 \left\| \nabla_{\mathbf{c}} \hat{p}_i \Big|_{(M, \mathbf{X}, R), f} \right\|^2 \quad (26)$$

for $i = x, y, z$. The coefficients σ_b^2 and $\sigma_{\mathbf{c}}^2$, which designate the (known) variances of the pre-estimated parameters, have been chosen in accordance with the remarks following Def. 5.

C. Settings of the calibration

We apply the calibration method to a single-axis magnetometer for which estimates of bias and scale factor are available to a precision characterized by standard deviations $\sigma_b \approx 1.4$ mG and $\sigma_{\mathbf{c}} \approx 1.4 \cdot 10^{-3}$. We confront the method to both simulated and real data, minimizing the (scalar) sensitivity separately for each of the three components of \mathbf{p} .

1) *Simulation*: We simulate the ambient magnetic field in navigation frame as modelled by its value at a chosen origin, $\mathbf{B}_0^n = (0.46, 0.0, 0.0)^\top$ G, and a uniform gradient $\nabla \mathbf{B}_0^n$ whose (Frobenius) norm is of order 45 mG/m. The model for the magnetic field is supposed to be perfectly known in the calibration algorithm. The calibration trajectory consists of 35 samples corresponding to non-uniformly chosen positions and attitudes of the body frame (to

⁵Having in mind a typical indoor environment, norm and direction of the magnetic field vary relatively by far less 1 along the calibration trajectory.

⁶For Hessian matrices $H_{\mathbf{p}, \mathbf{p}}$, we use the notations of in Sec. III-C.

TABLE II: Simulation results for the position error and sensitivity to the errors with respect to pre-estimated bias and scale factor values. The indicated scalar sensibility is the square root of $\Lambda = \sum_{i=x,y,z} \Lambda^{(i)} (\hat{f}^{(i)})$ with $\Lambda^{(i)}$ as in Eq. (15) and $\hat{f}^{(i)}$ the weight function minimizing $\Lambda^{(i)}$.

	OLS	Optimized weights
Error $\ \delta\mathbf{p}\ $ (mm)	15	0.05
Scalar sensitivity $\Lambda^{1/2}$ (mm)	15	0.15

which the magnetometer is attached). Positions and attitudes are also supposed to be known without error in the calibration algorithm.

For bias and scale factor, we choose the true values $b_* \approx -3.0$ mG and $\mathbf{c}_* = (1.0 \ 0.0 \ 0.0)$. Their pre-estimates b_0 and \mathbf{c}_0 are simulated by adding errors randomly chosen according to a Gaussian law with standard deviations as specified above.

2) *Real data*: Real data is obtained from a calibration trajectory confined to an indoor region allowing for position and attitude tracking by an optical motion capture. For this considered volume, the magnetic model has been determined beforehand. Harmonizing the data of motion capture with an on-board inertial measurement unit in the body reference frame, we are in the position to define the body frame origin as the position of the accelerometer and the body frame orientation by the accelerometer axes. The calibration parameters to estimate are then the position coordinates of the magnetometer in this frame. A reference position (at millimeter precision) is available by conventional metric measurements.

Errors in the bias b and the scale factors \mathbf{c} considered in this study dominate over the errors due to noise or systematic errors in the motion capture data and the magnetic field model. Focussing on the sensitivity to b and \mathbf{c} , a detailed characterization of the errors in position, attitude, and model parameters is not necessary. (Such errors may yet be included in the sensitivity measure in a separate study.)

D. Results

1) *Simulations*: Table II shows the results of the simulation study. The OLS method (*i.e.* a uniform weight function) yields a position $\hat{\mathbf{p}}$ with an error of 15 mm, in accordance with the sensitivity to bias and scale factor errors of also 15 mm (in units of their respective standard deviations). Minimizing this sensitivity to both bias and scale factor errors, it is reduced to below 0.15 mm, which is reflected by a position error of less than 0.05 mm, a precision that is difficult to achieve using conventional means.

2) *Real data*: The results for real-life data are shown in Table III. The position error using the conventional OLS method amounts to 43 mm, which is in magnitude twice the OLS error obtained in simulations. We may attribute

TABLE III: Experimental results for the position error and sensitivity to errors in pre-estimated bias and scale factor values. The indicated position errors is obtained by comparison with the conventionally measured magnetometer position (relative to the on-board accelerometer).

	OLS	Optimized weights
Error $\ \delta\mathbf{p}\ $ (mm)	43	4.6
Scalar sensitivity $\Lambda^{1/2}$ (mm)	20	0.1

this increased error to noise and systematic errors that have not been included in the simulation model.

Applying the weights obtained from our sensitivity minimization algorithms, we obtain a position that is accurate up to 5 mm in comparison with the (nominal) reference position. Minimization of sensitivity has thus been reduced the error by a factor of order 10. The residual position error of 5 mm can again be attributed to the errors in the motion capture data and the magnetic model.

E. Discussion

Our simulation shows that for sufficiently rich calibration trajectories, the sensitivity of the position calibration to errors in the pre-estimated parameters can be reduced to arbitrarily small values. Applying the method to data obtained in real experiments, we have achieved a net error reduction (by a factor of order 10), yet a residual position error of several millimeters remains. At this precision, our approach is reliable in the situation where conventional position measurements (including the simple use of a ruler) are unavailable, *e.g.* if the magneto-inertial measurement unit is hidden in a “black box”. In this case, we provide a *non-invasive* method to estimate the magnetometer position with an accuracy that is optimal with respect to errors in the pre-estimated calibration parameters.

For a further reduction of the position error, we may on one hand try and improve the performance of the reference data sets used in the calibration algorithm. These are the trajectory data set, which depends on the performance of the motion capture system, and the magnetic field model, which may be developed to a higher order and, in our case, would also benefit from a more performing motion capture system, we have used to map the local ambient field.

In a complementary approach, errors of the motion data and the magnetic field model may, too, be included into our sensitivity measure. In doing so, our approach may be extended beyond static errors (such those in bias and scale factor) to include also noise.

V. CONCLUSIONS

We have developed an optimized least-squares approach that minimizes sensitivities to errors in pre-estimated parameters, leading sometimes to complete vanishing. Such situations arise in calibration problems

in which a certain subset of parameters is already known (with limited accuracy) at a given step of the procedure.

We have tested our sensitivity-based approach in both simulation and experiment in the context of position calibration of magnetometers in an inhomogeneous magnetic field. In simulation, we have proven the validity of the approach. Our experimental result shows a significant error reduction. We have discussed how the residual error may further be reduced in future studies.

Our approach may finally be helpful in the design of a calibration process such as the conception of a calibration trajectory with minimal sensitivity to errors.

ACKNOWLEDGMENTS

We are grateful to ESIGELEC School of Engineering in Rouen-Madrillet, F-BP 10024 76801, for their expertise and support in the use of their optical tracking device.

APPENDIX

A. Least-squares optimization for the toy model of Sec. II

For a set measurements that are homogeneously distributed in the interval (θ_1, θ_2) , we consider for the calibration model of Eq. (2) the cost function

$$\int_{\theta_1}^{\theta_2} (M(\theta) - b_0 - \mathbf{c} \cdot R(\theta)^\top \mathbf{B}^n)^2 d\theta. \quad (27)$$

The bias in this cost function is considered fixed and pre-estimated with an error δb . Minimization of (27) yields the estimate

$$\hat{\mathbf{c}} = \left[\int_{\theta_1}^{\theta_2} (M(\theta) - b_0) \mathbf{B}^{n\top} R(\theta) d\theta \right] \cdot K(\theta_1, \theta_2) \quad (28)$$

with

$$K(\theta_1, \theta_2) = \left[\int_{\theta_1}^{\theta_2} R^\top(\theta) \mathbf{B}^n \mathbf{B}^{n\top} R(\theta) d\theta \right]^{-1}. \quad (29)$$

Note that if θ_1 and θ_2 span over a full interval of length 2π , Eq. (28) shows that $\hat{\mathbf{c}}$ is independant from b_0 and therefore insensitive to any possible error in it.

For \mathbf{c}_* the true value of the scale factor vector, the (noise-free) measurement is $M(\theta) = \mathbf{c}_* \cdot R(\theta)^\top \mathbf{B}^n + b_*$ and the LS estimate (28) contains an error

$$\delta \mathbf{c} = \hat{\mathbf{c}} - \mathbf{c}_* = -\delta b \left[\int_{\theta_1}^{\theta_2} \mathbf{B}^{n\top} R(\theta) d\theta \right] \cdot K(\theta_1, \theta_2). \quad (30)$$

The remaining integrations and matrix products are elementary and yield the results reported in Sec. II.

REFERENCES

- [1] Y. Adachi, M. Higuchi, D. Oyama, Y. Haruta, S. Kawabata, and G. Uehara, "Calibration for a multichannel magnetic sensor array of a magnetospinography system," *IEEE Transactions on Magnetics*, vol. 50, pp. 1–4, nov 2014.
- [2] C.-I. Chesneau, M. Hillion, and C. Prieur, "Motion estimation of a rigid body with an EKF using magneto-inertial measurements," in *2016 International Conference on Indoor Positioning and Indoor Navigation (IPIN)*, (Alcalá de Henares, Spain), oct 2016.
- [3] C.-I. Chesneau, M. Hillion, J.-F. Hullo, G. Thibault, and C. Prieur, "Improving magneto-inertial attitude and position estimation by means of a magnetic heading observer," in *2017 International Conference on Indoor Positioning and Indoor Navigation (IPIN)*, (Sapporo, Japan), sep 2017.
- [4] C.-I. Chesneau, R. Robin, H. Meier, M. Hillion, C. Prieur, "Calibration of a magnetometer array using motion capture equipment," *Asian Journal of Control*, Asian Control Association (ACA) and Chinese Automatic Control Society (CACSS) 2019, 21 (4), pp.1459-1469. 10.1002/asjc.2043. hal-02368023.
- [5] M. Díaz-Michelena, R. Sanz, M. F. Cerdán, and A. B. Fernández, "Calibration of qm-moura three-axis magnetometer and gradiometer," *Geoscientific Instrumentation, Methods and Data Systems*, vol. 4, no. 1, pp. 1–18, 2015.
- [6] D. N. Dyck and D. A. Lowther, "Automated design of magnetic devices by optimizing material distribution," in *IEEE Transactions on Magnetics*, vol. 32, no. 3, pp. 1188-1193, may 1996 doi:10.1109/20.497456.
- [7] J. Fogelquist and X. Lin, "Uncertainty-Aware Data Selection Framework for Parameter Estimation with Application to Li-ion Battery," *2022 American Control Conference (ACC)*, pp. 384-391, Atlanta, USA, jun 8-10, 2022.
- [8] C. Huang, G. Hendeby, I. Skog, "A Tightly-Integrated Magnetic-Field aided Inertial Navigation System", 8 pages, 2022.
- [9] M. Kok, J. D. Hol, T. B. Schön, F. Gustafsson, and H. Luinge, "Calibration of a magnetometer in combination with inertial sensors," in *2012 15th International Conference on Information Fusion*, (Singapore), pp. 787–793, July 2012.
- [10] V. Renaudin, M. Haris Afzal, G. Lachapelle, "Complete Triaxis Magnetometer Calibration in the Magnetic Domain," Hindawi Publishing Corporation, *Journal of Sensors*, Volume 2010, Article ID 967245, 10 pages. doi:10.1155/2010/967245.
- [11] K. Levenberg, "A method for the solution of certain non-linear problems in least squares," *Quarterly of Applied Mathematics*, vol. 2, pp. 164–168, jul 1944.
- [12] X. Li, Y. Wang, and Z. Li, "Calibration of tri-axial magnetometer in magnetic compass using vector observations," in *2015 IEEE 28th Canadian Conference on Electrical and Computer Engineering (CCECE)*, IEEE, may 2015
- [13] D. W. Marquardt, "An algorithm for least-squares estimation of nonlinear parameters," *Journal of the Society for Industrial and Applied Mathematics*, vol. 11, pp. 431–441, jun 1963.
- [14] K. Mohamadabadi and M. Hillion, "An automated indoor scalar calibration method for three-axis vector magnetometers," *IEEE Sensor Journal*, vol. 14, pp. 3076–3083, sep 2014.
- [15] H. Pang, S. Luo, Q. Zhang, J. Li, D. Chen, M. Pan, and F. Luo, "Calibration of a fluxgate magnetometer array and its application in magnetic object localization," *Measurement Science and Technology*, vol. 24, p. 075102, may 2013.
- [16] J. Schoukens, L. Ljung, "Nonlinear System Identification," *IEEE Control System Magazine*, pp. 28-99, dec. 2019. doi:10.1109/MCS.2019.2938121.
- [17] Y. Shin, D. Xiu, "Nonadaptive Quasi-Optimal Points Selection for Least Squares Linear Regression," *SIAM Journal on Scientific Computing*, vol. 38, pp. A385-A411, 2016. doi: 10.1137/15M1015868.
- [18] S. Turner, M. J. Hall, S. Harmon, and N. Hillier, "Calibration of a novel three-axis fluxgate gradiometer for space applications," *IEEE Transactions on Magnetics*, vol. 51, pp. 1–4, jan 2015.
- [19] D. Vissière, A. Martin, and N. Petit, "Using distributed magnetometers to increase imu-based velocity estimation into perturbed area," in *Conference on Decision and Control (CDC)*, (New Orleans, LA), pp. 4924–4931, 2007.
- [20] D. Yang, Z. You, B. Li, W. Duan, and B. Yuan, "Complete tri-axis magnetometer calibration with a gyro auxiliary," *Sensors*, vol. 17, no. 6, p. 1223, 2017.
- [21] T. Yoshida, M. Higuchi, T. Komuro, and H. Kado, "Calibration system for a multichannel squid magnetometer," in *Proceedings of 16th Annual International Conference of the IEEE Engineering in Medicine and Biology Society*, (Baltimore, MD, USA), nov 1994.
- [22] M. Zmitri, H. Fourati, C. Prieur, "Magnetic Field Gradient-Based EKF for Velocity Estimation in Indoor Navigation," in *Sensors*, no. 20, p. 5726. doi: 10.3390/s20205726.
- [23] M. Zmitri, H. Fourati and C. Prieur, "BiLSTM Network-Based Extended Kalman Filter for Magnetic Field Gradient Aided Indoor Navigation," in *IEEE Sensors Journal*, vol. 22, no. 6, pp. 4781-4789, 15 March 2015, 2022, doi: 10.1109/JSEN.2021.3091862.